AD-A036 386 PHYSICAL DYNAMICS INC TORRANCE CALIF F/G 20/4
AN ANALYTICAL STUDY OF THE EFFECT OF SURFACE ROUGHNESS ON THE S--ETC(U)
NOV 76 M A KOSECOFF, D R KO, C L MERKLE N00014-76-C-0967
UNCLASSIFIED PDT-76-131 NL

1 OF 1
ADA036386

END

DATE FILMED
3 - 77

PDT-76-131

FINAL REPORT

AN ANALYTICAL STUDY OF THE EFFECT OF SURFACE ROUGHNESS ON THE STABILITY OF A HEATED WATER BOUNDARY LAYER

NOVEMBER 1976

BY: MICHAEL A. KOSECOFF, DENNY R. S. KO, AND CHARLES L. MERKLE

SUBMITTED TO: OFFICE OF NAVAL RESEARCH
ARLINGTON, VIRGINIA

CONTRACT N00014-76-C-0967

PHYSICAL DYNAMICS, INC.
3838 CARSON STREET, SUITE 110
TORRANCE, CALIFORNIA 90503

PDT-76-131

FINAL REPORT

AN ANALYTICAL STUDY OF THE EFFECT OF SURFACE ROUGHNESS ON THE STABILITY OF A HEATED WATER BOUNDARY LAYER

By

Michael A. Kosecoff, Denny R. S. Ko, and Charles L. Merkle

November 1976

Supported by

Defense Advanced Research Projects Agency

and

Office of Naval Research

Under

Contract N00014-76-C-0967

UNCLASSIFIED

SECURITY CLASSIFICATION OF THIS PAGE (When Data Entered)

REPORT DOCUMENTATION PAGE

READ INSTRUCTIONS BEFORE COMPLETING FORM

1. REPORT NUMBER	2. GOVT ACCESSION NO. / 3. RECIPIENT'S CATALOG NUMBER
4. TITLE (and Subtitle): An Analytical Study of the Effect of Surface Roughness on the Stability of a Heated Water Boundary Layer.	5. TYPE OF REPORT & PERIOD COVERED: Final Report. 22 Apr 76 — 30 Sep 76
	6. PERFORMING ORG. REPORT NUMBER: PDT-76-131
7. AUTHOR(s): Michael A. Kosecoff, Denny R. S. Ko, and Charles L. Merkle	8. CONTRACT OR GRANT NUMBER(s): Contract N00014-76-C-0967
9. PERFORMING ORGANIZATION NAME AND ADDRESS: Physical Dynamics, Inc. 3838 Carson Street, Suite 110 Torrance, CA 90503	10. PROGRAM ELEMENT, PROJECT, TASK AREA & WORK UNIT NUMBERS
11. CONTROLLING OFFICE NAME AND ADDRESS: Office of Naval Research, Department of the Navy 800 North Quincy Street Arlington, VA 22217	12. REPORT DATE: Nov[illegible]976 / 13. NUMBER OF PAGES: 37 12 46p.
14. MONITORING AGENCY NAME & ADDRESS(if different from Controlling Office)	15. SECURITY CLASS. (of this report): Unclassified / 15a. DECLASSIFICATION/DOWNGRADING SCHEDULE

16. DISTRIBUTION STATEMENT (of this Report)

17. DISTRIBUTION STATEMENT (of the abstract entered in Block 20, if different from Report)

18. SUPPLEMENTARY NOTES

19. KEY WORDS (Continue on reverse side if necessary and identify by block number)

Boundary layer
Heating
Stability
Surface roughness
Transition

20. ABSTRACT (Continue on reverse side if necessary and identify by block number)

The onset of transition from laminar to turbulent flow in a high Reynolds number, water boundary layer has been investigated with emphasis on predicting the global effects of distributed surface roughness on transition. The particular approach which has been followed is to use the results of linear stability theory as an indicator of transition, but, for the initial results which are reported herein, only comparisons of the stability results themselves (not actual transition predictions) are given. The effects of surface roughness on transition have been

(cont'd p 1473B)

DD FORM 1473 (FACSIMILE)

UNCLASSIFIED 410 068

SECURITY CLASSIFICATION OF THIS PAGE (When Data Entered)

included by means of an existing phenomenological model for the effects of distributed roughness on the mean flow profiles. This model, which was originally developed for high Mach number, compressible boundary layers, has been applied without change to the present incompressible, water boundary-layer environment, and identical values of the required empirical constants have been used in both cases. Some important conclusions which can be obtained from the numerical results are that the presence of favorable pressure gradients and/or surface heating serve to make the boundary layer more susceptible to roughness, not only when compared in terms of the actual roughness height, k, but also when compared in terms of the roughness height to momentum thickness ratio, (k/θ). Further when the roughness is sufficiently large, its presence can change the effect of surface heat addition from a strongly stabilizing factor to a strongly destabilizing phenomena, indicating that heating on walls of sufficiently large roughness can be detrimental rather than helpful.

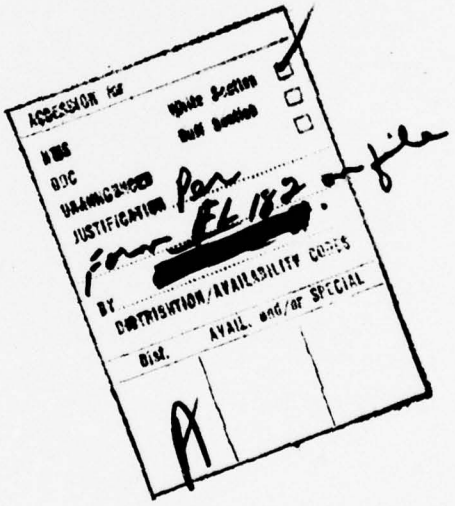

ABSTRACT

The onset of transition from laminar to turbulent flow in a high Reynolds number, water boundary layer has been investigated with emphasis on predicting the global effects of distributed surface roughness on transition. The particular approach which has been followed is to use the results of linear stability theory as an indicator of transition, but, for the initial results which are reported herein, only comparisons of the stability results themselves (not actual transition predictions) are given. The effects of surface roughness on transition have been included by means of an existing phenomenological model for the effects of distributed roughness on the mean flow profiles. This model, which was originally developed for high Mach number, compressible boundary layers, has been applied without change to the present incompressible, water boundary-layer environment, and identical values of the required empirical constants have been used in both cases. Some important conclusions which can be obtained from the numerical results are that the presence of favorable pressure gradients and/or surface heating serve to make the boundary layer more susceptible to roughness, not only when compared in terms of the actual roughness height, k, but also when compared in terms of the roughness height to momentum thickness ratio (k/θ). Further when the roughness is sufficiently large, its presence can change the effect of surface heat addition from a strongly stabilizing factor to a strongly destablilizing phenomena, indicating that heating on walls of sufficiently large roughness can be detrimental rather than helpful.

TABLE OF CONTENTS

LIST OF FIGURES

SYMBOLS AND NOTATION

A^+	"Van Driest" parameter in roughness model (*q.v.*)
C	Nondimensional viscosity
C_p	Specific heat
F	Similarity function for velocity
G	Similarity function for enthalpy
H	Enthalpy; shape factor
k	Effective roughness height; laminar thermal conductivity
k_T	Total/effective thermal conductivity
K_ε, K'_ε	Parameters in roughness model (*q.v.*)
p	Static pressure
Pr	Laminar Prandtl number
P_t	Turbulent Prandtl number
P_T	Effective Prandtl number
r_o	Radius of an axisymmetric body
Re_ℓ	Reynolds number based on the length scale ℓ
T	Static temperature
u	Local streamwise velocity component
v	Local normal velocity component
x	Streamwise coordinate
y	Coordinate normal to surface

SYMBOLS AND NOTATION (continued)

α	Complex wave number = $\alpha_r + i\,\alpha_i$
β	Falkner-Skan pressure gradient parameter
β_1	Parameter in roughness model (*q.v.*)
δ	Boundary layer thickness
δ^*	Displacement thickness
ε_H	Thermal diffusivity due to roughness
ε_M	Momentum diffusivity due to roughness
ΔT	$T - T_e$
η	Normal coordinate in Levy-Lees transformation
θ	*Momentum thickness*
Θ	$\Delta T/\Delta T_w$
μ	*Laminar molecular viscosity*
μ_T	Total/effective molecular viscosity
ν	*Laminar kinematic viscosity*
ξ	Streamwise coordinate in Levy-Lees transformation
ρ	Density
Ψ	Stream function for axisymmetric flow
ω	Real frequency
Ω	Nondimensional frequency

Subscripts

e	Evaluated at the boundary layer edge
k	Evaluated at the roughness height
w	Evaluated at the wall

1.0 INTRODUCTION

When a high Reynolds number vehicle moves through a quiescent fluid, viscous forces in the boundary layer accelerate the fluid near the vehicle's surface and leave it with a residual net momentum. For vehicles on which the boundary layer remains attached, this momentum represents nearly the entire drag of the vehicle. The total amount of momentum which is transferred to the surrounding fluid (and, hence, the drag of the vehicle) depends crucially on the character of the boundary layer. If the boundary layer is laminar, the amount of momentum deposited in the boundary layer is relatively small, but, if the boundary layer is turbulent, it is substantially larger. Since this drag must be overcome by the propulsive system, it behooves us to minimize, to as large an extent as practical, the amount of momentum which is transferred to the surrounding fluid. One particularly attractive method for achieving this objective is to employ boundary layer control techniques to delay transition from the laminar to the turbulent state. If the laminar boundary layer can be maintained over the entire vehicle (or nearly so), impressive performance improvements can be obtained.

In the past few years, substantial progress toward reaching this goal of a high Reynolds number, all-laminar vehicle has been reported. The incorporation of recent advances in boundary layer control techniques has allowed the feasibility of all-laminar, underwater vehicles to be demonstrated at practical body Reynolds numbers, at least in carefully controlled experimental situations. The ability to maintain these impressive performance improvements in a realistic environment or to extend them to even higher Reynolds numbers represents an important achievement which must still be demonstrated. The present report describes some initial results of a study which is aimed at determining how vehicles whose design is based on these advanced boundary-layer control techniques will perform in such realistic environments. In particular, the results in this report are centered on estimating appropriate levels of surface roughness which can be tolerated without negating the effects of the boundary layer control.

The two principal boundary layer control techniques which have been relied upon to delay transition in the experimental demonstrations noted above are body

shaping and surface heating. Body shaping is used to generate a favorable (negative) pressure gradient over large portions of the vehicle, thus providing a boundary layer which is strongly stable to disturbances. Surface heating is likewise strongly stabilizing in water boundary layers because of the simultaneous effects of the variation of the viscosity of water with temperature in conjunction with the relatively high Prandtl number of water. Experimental results have consistently shown that techniques such as these which serve to increase the stability of the boundary layer also serve to increase the transition Reynolds number. Some computations which show the magnitude of these two factors on stability and transition have been given by Gazley et al. (1976).

Quite obviously, any real surface is not perfectly smooth but contains some roughness. It is well known that surface roughness hastens boundary-layer transition, and, as will be shown herein, both favorable pressure gradients and surface heating tend to amplify the effects of roughness. Surface roughness may enter from a variety of sources, including imperfections arising from the manufacturing process and surface degradation with time due to external influences. It is of fundamental importance to assess the interactions between surface roughness and body shaping and heating with regard to their effect on transition. For example, it is anticipated that there should be a threshold roughness below which the transition Reynolds number is indistinguishable from that on smooth walls. It is important to determine whether this "smooth wall" range is wide or narrow, and whether the effects of roughness become evident gradually or catastrophically once this level has been exceeded. This roughness behavior can have important practical implications as regards the implementation of shaping and heating in real design problems where the degree of smoothness which is practically attainable is of concern. Further, it is important to identify acceptable roughness heights so that overly-conservative surface finishes are not specified.

The particular emphasis of the present report is to make a qualitative assessment of the mutual interactions between the effects of surface roughness and favorable pressure gradient and surface heating. The basic approach which is followed herein is to use the techniques of linear stability theory as a guide to understanding the complex phenomena which are encountered in the transition process,

and for quantitatively estimating the magnitude and direction of its movement under the influence of the various boundary layer parameters. The effects of favorable pressure gradient and surface heating on boundary layer stability (and transition) are automatically included in classical, parallel-flow stability theory; however, the effects of surface roughness are not so easily determined. The present results are based on a phenomenological model for the effects of surface roughness on the mean flow profiles, and, by inference, on the stability characteristics of a boundary layer. Thus, in the present work, the effects of roughness on boundary layer transition are incorporated through a distortion of the mean flow profiles. Although the model is founded upon experimental information, that information is admittedly meager, and full justification of the approach requires additional experimental verification. The fundamental postulate that the mean flow profiles over a rough wall are different from those which would be expected for a smooth wall is difficult to refute; the uncertainty lies in manner by which these distortions are included. Full details of the model are included in Section 2.0; some representative results and a qualitative assessment of the effects of roughness on the mean flow profiles are given in Section 3.0, and its effects on the stability characteristics are given in Section 4.0.

2.0 APPROACH

We begin by presenting a brief overview of possible types of surface roughness and then discuss some experimental results which show the mechanisms by which one particular type of roughness affects transition. Building upon this experimental background, we then discuss a postulated model for the effects of distributed roughness on the mean flow profiles. Subsequent sections incorporate this model into the mean flow, and finally, present the results of calculations of the stability characteristics of the modified mean flow.

2.1 Types of Roughness

Roughness may result from a variety of sources. The manufacture of a body may require polishing simply due to raw materials used; however, machining itself may also be a significant source of roughness. Additional new sources of roughness appear once the body is introduced into a real environment. For example, dust in air or comparable particles in water may adhere to the surface; impact with small particles may result in pitting; and chemical reactions between the surface material and the surrounding fluid may result in corrosion. Each different source can result in a different type of roughness.

In an attempt to bring some order into this situation, several categories of roughness can be identified for both analytical and experimental purposes. These include a single isolated protrusion, a few isolated protrusions (typically similar or identical in structure), and a closely packed regular or irregular array of protrusions (distributed roughness). In addition to these three-dimensional types of roughness, categories of a two-dimensional nature, including isolated cylindrical roughness elements (e.g., trip wires), and multiple cylindrical elements or wavy walls may also be encountered.

For each type of roughness, it is necessary to identify those parameters which suffice to characterize the roughness. Attempts to discriminate among roughness elements of different shapes have been reported by Schlichting (1968) for the case of turbulent flows through rough pipes. His categories include elements which are spheres, segments of sphere, cones, and "short angles." For the case

of distributed roughness, similar categorization of the shapes of the roughness elements is desirable, including whether the individual elements are similar in shape, or whether they are composed of a random assortment of shapes. However, some additional parameters also enter in the distributed roughness case. For example, the number of roughness elements per unit of surface area is very important, as is the height distribution of the elements. Either of these parameters could be used to define a continuous parametric space between distributed roughness and single isolated three-dimensional elements. Thus, if the number density of roughness elements were continuously decreased, the distributed roughness would approach a single (or, at least, multiple isolated) roughness element(s). Similarly, if the height distribution is continuously changed from one in which all elements are of identical heights to one where a few elements are noticeably bigger than the other smaller ones, these few tall elements could again act as isolated roughness elements.

As noted above, the analysis in this report is restricted to distributed surface roughness, but in an attempt to retain only the most dominant effects of the roughness, the present analysis characterizes the roughness by a single parameter, the effective roughness height, k. Certainly, this is an oversimplification; the number density, the individual shapes, and the height distribution of the elements are also important, but these details are ignored for the present. Using only a single parameter to characterize the roughness should still give meaningful qualitative results for many distributed roughness cases. The radical deviations from distributed roughness (and, in particular, those which begin to act as individual roughness elements) can not be treated with the present analysis. The inclusion of their effects requires additional considerations.

2.2 The Effects of Surface Roughness: Experimental Background

Most experimental work relating to the effects of roughness on transition has concentrated on the relationship between the various types of roughness and the transition Reynolds number, rather than on the microscopic physics in the neighborhood of a roughness element and how it affects the transition mechanisms. A concise summary of such results may be found in the review article by Tani (1969).

It should be noted that even these "macroscopic" experiments are generally concerned with either a single cylindrical (two-dimensional) roughness element, or an isolated protuberance (three-dimensional element), rather than with distributed surface roughness. For the case of distributed roughness, even the macroscopic information concerning the effects of roughness on the transition location is limited, and data showing the effects of heat transfer, or pressure gradient, is even more difficult to find.

One experiment in which the detailed effects of roughness on the movement of transition were studied is the one by Klebanoff and Tidstrom (1972). They observed the interaction between roughness and the mean velocity profile in an experiment wherein a cylindrical, two-dimensional roughness element was placed on the surface of a flat plate at a stream-wise location at which the boundary layer was still laminar, but was sufficiently thick to submerge the cylinder completely. Measurements taken downstream of the cylinder indicated that fluctuations inside the boundary layer were amplified or damped as they were swept downstream, depending on their frequency. Comparisons with computations from flat plate linear stability theory showed that the experimentally measured amplification rates were much higher than the values which would be predicted from smooth-wall theory; however, when the predicted amplification rates were computed from the measured mean velocity profiles (which were distorted from the Blasius shape by the presence of the wire), the results were in good agreement with the measured growth rate.

In addition to this increased amplification rate, which indirectly increased the fluctuation level, Klebanoff and Tidstrom found that the roughness element also served as a direct source of disturbances by introducing additional fluctuations in the laminar boundary layer. Consequently, their findings can be summarized by noting that roughness affects transition in the following two ways:

1. The presence of surface roughness alters the mean velocity profiles in such a manner that disturbances in the laminar boundary layer are amplified at a faster rate.
2. The presence of surface roughness generates additional disturbances in the boundary layer and, hence, changes the initial disturbance level before amplification begins.

These experimental observations have been used as the basis for our phenomenological model of the effects of distributed roughness on transition as outlined below.

2.3 Modeling the Effects of Distributed Surface Roughness

The experimental evidence of Klebanoff and Tidstrom, which was described above, clearly identifies the mechanisms by which a single two-dimensional roughness element causes transition to move forward. Similar detailed experimental information concerning the mechanisms through which distributed roughness affects the location of transition is completely lacking, but it is to be expected that distributed roughness would likewise affect the location of transition through the same two basic mechanisms: distortion of the mean flow profile, and generation of additional disturbances. Following the previous work of Merkle, Kubota, and Ko (1974), we have represented the assumed distortion of the mean flow by distributed roughness in terms of a simple phenomenological model. In the model, it is assumed that distributed roughness elements are spaced closely, compared to the characteristic wavelength of the boundary-layer disturbances. Further, the model views the flow over the many roughness elements as being unsteady in nature, similar to that commonly observed behind isolated bodies at intermediate Reynolds numbers. This postulated unsteadiness could occur in the form of either a vortex street or wake turbulence. In an integrated sense, these unsteady velocity fluctuations serve near the wall as a source of augmented momentum and heat transfer. These augmented transfer rates are modeled by local eddy diffusivities. In this fashion, the intractable flow field which is generated by the extremely complicated physical surface is circumvented by considering a statistical average which yields an "equivalent" behavior over a smooth surface. Effectively, a "turbulent roughness layer" with a thickness of the effective roughness height is assumed to be imbedded within the ordinary laminar boundary layer.

Quite naturally, this simple model does not faithfully reproduce the detailed flow field in this turbulent roughness layer; the complexities of the flow near an actual rough wall are far too great to attempt to describe completely. The model does, however, strive to incorporate the dominant effects of the most important processes which occur in the wall region, and it is felt that these

will have a greater influence on the global behavior of transition than the inconsistencies in the details of the flow in the immediate vicinity of the roughness. The model was originally empirically adjusted to match the experimental results of Feindt (1957) for the effects of distributed roughness on transition in the presence of favorable and unfavorable pressure gradients (Merkle, Kubota, and Ko, 1974), and it has since been used to predict the correct qualitative behavior of the (individual and simultaneous) effects of strong favorable pressure gradients, wall cooling, surface mass addition, and distributed surface roughness in compressible boundary layers. Complete justification and continued improvements of the model must await detailed experimental measurements of the flow field in the presence of distributed roughness.

The enhanced momentum transfer which is postulated to occur near the surface is represented by a momentum diffusivity, ε_M, while the analogous heat transfer is given by a thermal diffusivity, ε_H. The momentum diffusivity is expected to be significant near the wall, but it is expected to vanish for distances which are large compared to the roughness height, k. In mathematical form, the diffusivity is expressed in terms of a representative magnitude, ε_{max}, and a function, $F(y/k)$, which is of the order of unity near the wall, and goes to zero for $y >> k$. One such function which has this behavior is the Gaussian function, and we have defined the momentum diffusivity in terms of it as

$$\varepsilon_M = \varepsilon_{max} e^{-\beta_1 (y/k)^2}, \quad \beta_1 = \mathcal{O}(1)$$

where the constant β_1 is required to be of order unity so that the width of the region of amplified momentum transfer is similar to the roughness height. (In fact, $\beta_1 = 1.0$ was used for our calculations.) To determine a reasonable estimate for ε_{max}, analogous mechanisms for which experimental data are available were considered. Consideration of a turbulent wake [Merkle, Kubota, and Ko (1974) and Schlichting (1968)] have led to

$$\varepsilon_{max} = K'_\varepsilon \nu_k Re_k$$

where the roughness Reynolds number, Re_k, is defined in terms of the velocity, u_k, and the kinematic viscosity, ν_k, evaluated at the roughness height $y = k$:

$$Re_k = \frac{u_k\, k}{\nu_k} .$$

The empirical constant K_ε' is expected to have the magnitude $K_\varepsilon' = \mathcal{O}(0.1)$. Furthermore, it is expected that momentum transfer by the unsteady, roughness-induced velocities has some threshold Reynolds number below which the flow is completely stable so that no "turbulent" momentum transfer takes place in the region near the wall (experimental results show that the flow field over an isolated body is completely stable up to some particular Reynolds number, after which unsteadiness begins). This threshold Reynolds number has been introduced into the model by allowing the coefficient K_ε' to have a Van Driest-type dependence on the local Reynolds number:

$$K_\varepsilon' = K_\varepsilon \left[1 - \exp(-Re_k/A^+)\right]$$

Based on experimental results taken from bodies in undisturbed flow, it is expected that this threshold Reynolds number is of the order of 40 (corresponding to the Reynolds number at which the vortex street behind a cylinder begins).

To summarize, the momentum diffusivity due to roughness is given by

$$\varepsilon_M = K_\varepsilon \nu_k Re_k \left\{1 - e^{-Re_k/A^+}\right\} e^{-\beta_1 (y/k)^2} .$$

For all the calculations reported here, the three constants in the model were set equal to their order of magnitude estimates described above. Thus, these constants were given the values,

$$K_\varepsilon = .094$$

$$A^+ = 40$$

$$\beta_1 = 1$$

Finally, the thermal diffusivity due to the surface is defined in terms of a turbulent Prandtl number, P_t,

$$\varepsilon_H = \varepsilon_M / P_t .$$

For all calculations reported herein, the turbulent Prandtl number was given the value of unity. The values for these four constants are identical to those chosen by Merkle, Kubota, and Ko (1974) and by Merkle (1976) for compressible rough wall boundary layers. None of the constants nor any of the assumptions in the model have been changed to apply the analysis to boundary layers in water.

The total or effective viscosity and thermal conductivity are given, respectively, by

$$\mu_T = \mu + \rho\varepsilon_M$$

$$k_T = k + \rho C_p \varepsilon_H$$

Here μ and k are the usual viscosity and thermal conductivity, ρ is the density, and C_p is the specific heat. The effect of the enhanced diffusivities is to decrease the velocity near the wall and to make the temperature profile thicker. Qualitative graphs illustrating this are shown in Figure 1. The total diffusivities, reflecting the sum of the laminar diffusivity and an "enhanced" contribution due to the presence of surface roughness, are shown schematically in Figure 2. Near the wall the total diffusivity is large, but at heights greater than the roughness height the usual laminar value is regained. Note from Figure 1 that when the velocity near the wall decreases sufficiently, the mean profile develops a point of inflection and is inviscidly unstable.

The above equations and diffusivities provide all the additional information needed to incorporate the effects of distributed surface roughness into the calculation of the distorted mean profiles in water, including the presence of heating and pressure gradients. Calculations of this nature are described in the following section, and the subsequent section contains the results of a stability analysis of the deformed profiles.

3.0 MEAN FLOW ANALYSIS

As noted by Klebanoff and Tidstrom (1972), one of the mechanisms by which roughness influences transition is through the distortion of the mean flow profiles. Having discussed how the effects of distributed surface roughness are to be modeled, we proceed to the development of the specific equations used for the mean flow and indicate the results attained.

3.1 Theory

The equations for a compressible, laminar boundary layer about an axisymmetric body of radius r_o are:

Conservation of mass

$$\frac{\partial}{\partial x} (\rho u r_o) + \frac{\partial}{\partial y} (\rho v r_o) = 0$$

Conservation of momentum (axial component)

$$\rho u \frac{\partial u}{\partial x} + \rho v \frac{\partial u}{\partial y} = - \frac{\partial p}{\partial x} + \frac{\partial}{\partial y} \left(\mu_T \frac{\partial u}{\partial y} \right)$$

Conservation of energy

$$\rho u \frac{\partial H}{\partial x} + \rho v \frac{\partial H}{\partial y} = \frac{\partial}{\partial y} \left[\frac{k_T}{C_p} \frac{\partial H}{\partial y} + \frac{1}{2} \left(\mu_T - \frac{k_T}{C_p} \right) \frac{\partial u^2}{\partial y} \right]$$

Note that the usual viscosity, μ, and conductivity, k, have been replaced by their rough-wall counterparts, μ_T and k_T. The temperature, T, which is needed to evaluate the viscosity and thermal conductivity, can be calculated from the stagnation enthalpy, H, according to

$$H = C_p (T - T_{ref}) + \tfrac{1}{2} u^2$$

since the specific heat of water is essentially constant in the region of interest. (T_{ref} is merely a reference temperature which does not affect the calculations.)

Although these partial differential equations could be solved directly (using an appropriate numerical procedure), their solutions would depend on the specific

body shapes and pressure distributions which were used, whereas, for these initial results, we are more interested in obtaining a qualitative description of the movement of the transition location in response to various heights of surface roughness. Accordingly, we have chosen to work with the similarity equations rather than the full partial differential equations. The similar form of the equations are somewhat simpler to solve (since they are ordinary differential equations), but they also make it much easier to parameterize the numerous variables in the problem, and, thus, to obtain a more rapid understanding of the global effects of distributed roughness on transition, as predicted by the model. Future calculations are planned, however, in which the onset of transition on realistic bodies, will be predicted. For these future calculations, the full partial differential equations will be solved by means of a standard numerical method.

It is worth noting that the axisymmetric nature of the geometry of the underwater body enters the analysis automatically through the mean flow equations. This results in significant differences between axisymmetric and planar, two-dimensional boundary layers (e.g., the growth rate of the boundary-layer thickness). By contrast, it is an established fact that the form of the stability or disturbance equations (discussed in the next section) is the same for axisymmetric and planar, two-dimensional flows; however, the coefficients differ since they are derived from different mean flow equations.

To determine the equations for similarity solutions corresponding to axisymmetric flow, we make use of the Levy-Lees transformation (Hayes and Probstein, 1959)

$$\xi(x) = \int_0^x \rho_e \mu_e u_e r_o^2 dx$$

$$\eta(x,y) = \frac{u_e r_o}{\sqrt{2\xi}} \int_0^y \rho \, dy$$

The subscript "e" here is used to denote evaluation at the edge of the boundary layer. For axisymmetric flow there exists a stream function, Ψ, which, for the similarity solution, can be written as

$$\Psi = \frac{\sqrt{2\xi}}{\rho_e r_o} F(\eta).$$

Using the standard methods, the velocity can then be computed from

$$u = u_e F'(\eta),$$

where, here the prime denotes differentiation with respect to eta. Similarly, the total temperature can be expressed in terms of the similarity function, G, as

$$G(\eta) = H/H_e.$$

Then, by introducing the local non-dimensional viscosity and the effective Prandtl number,

$$C = \mu_T/\mu_e, \quad P_T = C_p \mu_T / k_T$$

along with the Falkner-Skan pressure gradient parameter,

$$\beta = \frac{2\xi}{u_e} \frac{du_e}{d\xi},$$

the relevant equations become

$$(CF'')' + FF'' + \beta\left[\frac{\rho_e}{\rho} - (F')^2\right] = 0$$

$$\left(\frac{C}{P_T} G'\right)' + FG' = \frac{2\xi F' G}{H_e} \frac{dH_e}{d\xi} + \frac{u_e^2}{H_e} \left[\left(\frac{1}{P_T} - 1\right) CF'F''\right]'$$

We are able to make several simplications based on the fact that we are interested in low-speed flow in a heated water boundary layer:

- water is essentially imcompressible and $\rho \equiv \rho_e$
- the free stream enthalpy is constant and hence $\frac{dH_e}{d\xi} = 0$
- because u_e is small and the specific heat of water is large, $u_e^2/H_e \ll 1$ for only moderate heating.

The system of equations actually used to generate the mean flow profiles thus simplifies to

$$(CF'')' + FF'' + \beta[1 - (F')^2] = 0$$

$$\left(\frac{C}{P_T} G'\right)' + FG' = 0$$

The first of these equations is coupled to the second through the dependence of viscosity and the roughness model on temperature. The system is completed by specifying the boundary conditions at the wall,

no-suction, no-slip conditions: $F(0) = F'(0) = 0$

prescribed wall temperature: $G(0) = G_w$;

and the free stream values which are approached at the edge of the boundary layer,

$F'(\eta) \to 1$, $G(\eta) \to 1$ as $\eta \to \infty$.

These equations have been integrated numerically by means of a standard Runge-Kutta technique.

We note in passing that these boundary conditions for the rough-wall problem are identical to those for the smooth wall problem (i.e., they are specified at $y = 0$ rather than on the actual, irregular surface). Since we are working with boundary layer equations, such an approximation at first glance appears acceptable; it is acceptable to treat an irregular surface as a plane, so long as the radius of curvature is larger compared to the boundary layer thickness. However, closer inspection reveals that the local radius of curvature of the surface is of the order of the roughness height, so that not only the boundary layer curvature corrections, but also the complete elliptic equations, should be used in this region. The requirement for the elliptic equations is, of course, a statement that the pressure is no longer impressed by the outer flow field, but that it becomes a local variable which must be allowed to vary both along and across the boundary layer. Despite these many small scale fluctuations, the spirit of the present analysis is to attempt to include the global effects of these local pressure perturbations through a phenomenological model in much the same way that local (turbulent) pressure fluctuations in a turbulent boundary layer are ignored in the computation of the mean flow.

For completeness, we note that the physical properties of water which were used in the present analysis were computed from the formulas suggested by Lowell and

Reshotko (1974). After a review of the literature for empirical expressions for the dependence of the viscosity and thermal conductivity of pure water on temperature, they recommended the following expressions:

$$\log_e (\mu/\mu_{20^oC}) = \frac{-2.302585}{T - 164} \left| 1.37023 + 8.36 \times 10^{-4} (T - 293) \right| (T - 293)$$

and

$$k = 10^4 \left\{ -9.90109 + 0.1001982\, T - 1.873892 \times 10^{-4}\, T^2 + 1.03957 \times 10^{-7}\, T^3 \right\},$$

where the reference viscosity is $\mu_{20^oC} = 1.005$. These expressions have been chosen so that the first derivatives, as well as the functions themselves, can be represented with a high degree of accuracy. In these formulas, the temperature T is prescribed in degrees Kelvin, the molecular viscosity μ is given in centipoise, and the thermal conductivity k is given in ergs per centimeter-second-degree Kelvin.

The effects of roughness enter through the use of μ_T and k_T in place of μ and k, respectively. By setting the roughness height to zero (or to a very small value) and equating the free stream and wall temperatures, it was possible to generate the conventional (adiabatic) Falkner-Skan solutions as a verification of the reliability of the code used to solve the similarity equations. In order to verify the code when there is a heat flux across the boundary layer, use was made of a relation between G and F for a (smooth) flat plate (i.e., $\beta = 0$) established by Pohlhausen (Curle, 1962). If $\Theta = (T - T_w) / (T_e - T_w)$, where T_w is the wall temperature, then Θ is given in terms of the Blasius profile F and the free stream Prandtl number Pr by

$$\Theta(\eta) = \alpha_o(Pr) \int_0^\eta \left\{ \frac{F''(\eta)}{F''(0)} \right\}^{Pr} d\eta$$

The function $\alpha_o(Pr)$, which has been tabulated, is given by

$$\alpha_o(Pr) = \left\{ \int_0^\infty \exp\left(-Pr \int_0^\eta F d\eta \right) d\eta \right\}^{-1}$$

and is reasonable well approximated by

$$\alpha_o(Pr) \simeq 0.664 (Pr)^{1/3}.$$

3.2 Results

A number of mean velocity and temperature profiles were calculated for parametric values of heating, pressure gradient, wall temperature, and effective roughness height. The overall results found are exemplified by the profiles for a flat plate ($\beta = 0$) which appear in Figure 3. The boundary layer thickness δ was taken to be the value of y where $u/u_e = .999$. Normalized velocities u/u_e and temperatures $\Theta = \Delta T/\Delta T_w$ are shown as function of y/δ for various values of the non-dimensional roughness height, k/θ. Here $\Delta T = T - T_e$, $\Delta T_w = T_w - T_e$, k is the effective roughness height, and θ is the momentum thickness of the distorted mean profile. The results quantitatively verify the qualitative profiles anticipated in Figure 1.

As roughness increases, the gradients of both the velocity and temperature profiles decrease near the wall as a consequence of the increased diffusivity there. Near the boundary layer edge, the profiles are not influenced greatly by the diffusivities. This tends to introduce an inflection point into the mean velocity profile, making the profile more unstable from an inviscid point of view. Because of the large Prandlt number of water [$Pr = \mathcal{O}(10)$], the smooth wall thermal boundary layer is considerably thinner than the velocity boundary layer. Since the "turbulent Prandlt number" P_t is of order unity, the effect of roughness is experienced equally by both the velocity and temperature profiles near the wall. The consequence of this is that a moderate degree of roughness tends to drive the thickness of both the velocity boundary layer and the temperature boundary layer towards each other.

Note that for the flat plate case, the $k/\theta = 0$ and $k/\theta = .3$ the curves are essentially coincident. This suggests that a certain range of roughness may be considered equivalent to a smooth wall. For $k/\theta = 1$ the curves deviate modestly from the smooth wall profiles, and for $k/\theta = 2$ they deviate substantially. However, stability calculations presented in the next section demonstrate that only a modest deviation from the smooth wall profile is needed to result in a drastic change in the stability characteristics.

4.0 STABILITY ANALYSIS

In the previous section we presented a model to evaluate how distributed surface roughness alters the mean flow profiles. These distorted profiles should have different stability characteristics which will influence the onset of the transition phemomena. The transition criteria which we plan to utilize in future analyses, described below, is primarily based upon spatial amplification rates.

It is appropriate to recall here an alternative transition mechanism, other than the deformation of the mean profiles, as it relates to stability theory. As previously noted, Klebanoff and Tidstrom noted that roughness may introduce additional disturbances into the flow, changing the spectral content. If we postulate that transition occurs when a critical amplitude has been attained, it follows that when the initial amplitudes present are larger, transition will occur for a smaller value of the amplification ratio. This could be incorporated into "e^n" transition criterion by connecting the appropriate choice of "n" to the nature of the disturbance spectrum. We believe that this does not violate the spirit in which Smith and Gamberoni (1956) intended the criteria to be used. The calculations involved in an "e^n" type prediction derive directly from stability theory.

4.1 Theory and Procedure

The flow in a boundary layer can be decomposed into the sum of a mean flow and disturbances. If the disturbances are sufficiently small, the relevant equations can be linearized. If, further, one makes a parallel flow assumption, i.e., that the mean profiles and the pressure gradient vary slowly in the axial direction, then the disturbances can be decomposed into components of the form

$$\phi'(x,y,t) = \hat{\phi}(y)e^{i(\alpha x-\omega t)}$$

(Recall that, from a structural point of view, the disturbance equations for axisymmetric and planar, two-dimensional flows are identical, differing only in the evaluation of the coefficients from the mean flow profiles.) This results in a system of ordinary differential equations for functions of y. To study spatial stability, which is the focus of this report, the frequency ω is taken to be real and prescribed. Since the disturbance or stability equations, as well as the boundary conditions, are linear and homogeneous, nontrivial solutions are only

possible for complex wave numbers α which are eigenvalues of the system. Writing

$$\alpha = \alpha_r + i\,\alpha_i$$

we can express the local spatial amplification rate for a disturbance of a given frequency as $(-\alpha_i)$. Thus, once the mean profiles are known, it is possible to integrate the linear stability equations at each stream-wise location (or Reynolds number) to obtain the local amplification rate associated with each individual frequency component.

The indicated integration has been carried out using a numerical code developed by Lowell and Reshotko (1974), after making appropriate modifications so that it accepts the mean flow profiles we have generated. Modifications to include terms introduced into the stability equations by the enhanced viscosity have not been made at the present. It is anticipated that their effects on the results would be smaller than those caused by the distortions of the mean flow profile. The code uses an iterative method and incorporates an orthogonalization procedure to minimize parasitic error growth. The equations include temperature fluctuations and reflect the variation of viscosity and thermal conductivity with temperature, using the analytic expressions indicated in the previous section.

Nondimensional frequencies are prescribed:

$$\Omega = \omega \frac{\nu_e}{u_e^2}$$

Eigenvalues α were calculated as a function of Ω, Re_θ, β, ΔT_w, and k/θ (non-dimensional roughness height). This constitutes a five-dimensional parameter space, and so it was necessary to choose values carefully in order that results could be attained within reasonable time and financial constraints. For qualitative assessment, an ambient water temperature of 59°F was used for all calculations. Values of β chosen were -0.05 (adverse pressure gradient, $dp/dx > 0$), 0.0 (flat plate, $dp/dx = 0$), and 0.2 (favorable pressure gradient, $dp/dx < 0$). Re_θ was taken as an indicator of position and was held constant for each β. To illustrate the relative insensitivity resulting from this choice over Re_{δ^*} or Re_δ, plots of $H = \delta^*/\theta$ and δ/θ are given for the flat plate as a function of k/θ in Figure 4. Values of Re_θ were chosen so that, for the adiabatic smooth wall, Re_θ (or Re_{δ^*}) would lie approximately in the region of maximum instability. [(Reference can be made to the spatial stability maps generated by Wazzan, Okamura, and Smith (1968).]

The values are

β	Re_θ	Re_{δ^*} ($\Delta T_w = 0$, $k/\theta = 0$)
-0.05	224	600
0	385	1000
0.2	2103	5071

As noted in the introduction, the calculations performed are intended to be used for transition prediction. A cumulative amplification ratio can be calculated from the stability analysis according to

$$A/A_o = \exp\left\{-\int_{x_o}^{x} \alpha_i \, dx\right\}$$

where $A_o(\omega)$ and $A(\omega)$ are, respectively, the initial and local amplitudes of a disturbance with frequency ω. The e^n transition criterion which has been developed by Smith and Gamberoni (1956) predicts that the onset of transition will occur when this amplification ratio has reached a critical level

$$\left(A/A_o\right)_{crit} = e^n$$

for some frequency. Previous experience with adiabatic boundary layers indicates that the parameter n is generally of order 9 or 10.

4.2 Results

The principal results of the stability calculations are illustrated in Figures 5 through 10, which show the dependence of the nondimensional amplification rates ($-\alpha_i\theta$) as a function of Ω, the frequency, for $\beta = 0$ ($Re_\theta = 385$), $\beta = 0.2$ ($Re_\theta = 2103$), and $\beta = -0.05$ ($Re_\theta = 224$). The figures occur in pairs for each value of β. The first shows curves for a variety of nondimensional roughness heights when $\Delta T_w = 0^oF$; the second of each pair shows the same for both $\Delta T = 0^oF$ (solid lines) and $\Delta T = 30^oF$ (dashed lines).

Insofar as the curves are qualitatively similar in shape, it seem reasonable to characterize each by the peak amplification rate $(-\alpha_i\theta)_{max}$. With this simplification, there still remain three parameters whose interrelations we wish to

study, *viz.* k, ΔT_w, and β (or dp/dx). We accomplish this by fixing β and then generating two types of plots for each β: curves showing $(-\alpha_i\theta)_{max}$ as a function of k/θ for various values of ΔT_w (Figures 11, 12, and 13), and curves showing $(-\alpha_i\theta)_{max}$ as a function of ΔT_w for fixed values of k/θ (Figures 15, 16, and 17).

Figures 5, 7 and 9 demonstrate the anticipated result that the level of instability increases as the roughness increases in the absence of heating. It is also worthwhile noting that the range of unstable frequencies expands as roughness is increased. When heating is present (Figure 6, 8, and 10) a smooth wall is stabilized to some degree, as previously known. However, roughness plays a significant role in modifying this behavior. Initially there is a range of values for which a rough wall is indistinguishable from a smooth wall; a further increase in roughness then results in a moderate lessening of the stablizing effects of added heat. However, once the roughness height surpasses a critical value, heating exhibits a marked destabilizing effect on the boundary layer. Figures 11, 12, and 13 present these results in a more succinct fashion. From these figures it is possible to interpolate values of k/θ which correspond, qualitatively, to negligible, moderate, and drastic changes in the stability characteristics. Appropriate values are tabulated in Figure 14. These data permit us to draw some conclusions about the influence of a pressure gradient in the presence of roughness. Specifically, the more favorable the pressure gradient (i.e., as β increases), the narrower is the range of roughness heights for which a wall may be treated as smooth. Also, the more favorable the pressure gradient, the smaller are the criteria for what constitutes "critical roughness" beyond which there is a drastic tendency to destabilize.

Figures 15, 16, and 17 indicate that, for a given pressure gradient and roughness height, there exists an "optimal" amount of heating which stabilizes the boundary layer as much as possible, and a maximum amount beyond which heating only destabilizes. Clearly the former parameter is of principal interest. For sufficiently large roughness, the "optimal" amount of heating turns out to be no heating at all.

5.0 SUMMARY AND CONCLUSIONS

An analysis has been conducted to estimate the interrelations among the effects of heating, shaping, and particularly distributed surface roughness on the transition characteristics of high Reynolds number boundary layers in water. The estimates of the behavior of the transition location have been based upon the results of linear stability theory. The effects of distributed surface roughness have, in turn, been included in the stability analysis by means of a phenomenological model for the effects of roughness on transition. The model visualizes that roughness affects the location of transition by causing a distortion in the mean flow profile (from its smooth-wall shape) in such a manner as to alter its stability characteristics.

The model which has been used for these incompressible, water boundary layer predictions is identical to one previously developed and used for compressible, air boundary layers. For the case of compressible boundary layers, the model has been demonstrated to predict the correct qualitative trends for the effects of rougness on transition, as well as for the individual and simultaneous effects of streamwise pressure gradients, surface heat transfer, surface ablation, and Mach number, in the presence of roughness. Similar predictions for the mutual interaction between surface roughness, surface heat transfer and pressure gradient in water boundary layers are given in the present report. The present results indicate that the effects of these other parameters on transition can be qualitatively different in the presence of roughness as compared to their behavior on smooth walls. (As an example, heating, which is strongly stablizing in the presence of smooth walls, becomes strongly destablizing on rough walls.) Although experimental results to validate these predictions are presently lacking, it is noted that the model predicts similar reversals in the effects of a given parameter on transition in the presence of rough, as compared to smooth, walls for air boundary layers, and these predictions have been supported by a large bulk of experimental observations.

Some specific conclusions and observations about the roughness model and about the present predictions of the effects of roughness on transition are outlined below:

1. Roughness represents a powerful destabilizing influence in a boundary layer. The roughness model predicts that there is a range of roughness heights for which boundary layers behave almost as if they were on a smooth wall, but above this "threshold" roughness level, the effects of roughness quickly grow to where they completely dominate the stability and transition characteristics of the boundary layer.

2. In the presence of favorable pressure gradients, this threshold roughness level (when measured in terms of k/θ) is considerably smaller than for a flat plate. This trend continues to unfavorable pressure gradient boundary layers where the threshold roughness level is greater than for a flat plate.

3. As the roughness height is increased, the stabilizing effects of both favorable pressure gradient and heating on the growth of disturbances in the boundary layer is diminished, and when the surface roughness is sufficiently large, the effects of heating no longer serve to stabilize the boundary layer, but actually serve to destabilize it.

4. The present model for the effects of distributed surface roughness on the stability/transition characteristics of a boundary layer must certainly be tested against a well-controlled laboratory experiment which clearly identifies the mechanisms whereby roughness affects transition. Without the availability of such a check case, there are a number of minor improvements which could be made to the model. For example, the effects of the initial disturbances which are generated by the roughness elements could be included, and the effects of the enhanced viscosity could be incorporated directly into the stability calculations. The magnitude of such effects is, however, expected to be minor and is not considered to have major effects of the movement of the transition location due to roughness.

5. Finally, it is noted that the present roughness model is applicable only to distributed surface roughness and cannot be applied (without modification) to predict the effects of individual three-dimensional roughness elements, or two-dimensional roughness of the "wavy-wall" type.

REFERENCES

Curle, N. (1962), The Laminar Boundary Layer Equations, Oxford University Press, London.

Feindt, E. G. (1957), Untersuchungen über die Abhängigkeit des Umschlages laminar-turbulent von der Oberflächenrauhigkeit und der Druckverteilung, Gesellschaft, Vol. 50, pp. 180-203.

Gazley, Jr., C., Aroesty, J., King, W. S., Van Driest, E. R. (1976), Hydrodynamic Considerations in the Design of Small Submersible Vehicles (U), R-1866-ARPA, Rand, Santa Monica, CA (Confidential).

Hayes, W. D. and Probstein, R. F. (1959), Hypersonic Flow Theory, Academic Press, New York.

Klebanoff, P. S. and Tidstrom, K. D. (1972), "Mechanism by which a Two-Dimensional Roughness Element Induces Boundary-Layer Transition," *Phys. Fluids*, Vol. 15, No. 7, pp. 1173-1188.

Lowell, R. L. and Reshotko, E. (1974), Numerical Study of the Stability of a Heated Water Boundary Layer, FTAS TR 73-93, Case Western Reserve University, Cleveland, OH.

Merkle, C. L. (1976), Stability and Transition in Boundary Layers on Reentry Vehicle Nosetips, Flow Research Report No. 71, Kent, WA.

Merkle, C. L., Kubota, T., and Ko, D. R. S. (1974), An Analytical Study of the Effects of Surface Roughness on Boundary-Layer Transition, AFOSR-TR-75-0190, Flow Research Report No. 40, Kent, WA.

Schlichting, H. (1968), Boundary Layer Theory, Sixth Edition, McGraw-Hill, New York.

Smith, A. M. O. and Gamberoni, N. (1956), Report ES-26388, Douglas Aircraft Company, Long Beach, CA.

Tani, I. (1969), "Boundary-Layer Transition," Annual Reviews of Fluid Mechanics, Vol. 1, Annual Reviews, Inc., Palo Alto, CA.

Wazzan, A. R., Okamura, T. T., and Smith, A. M. O. (1968), Spatial and Temporal Stability Charts for the Falkner-Skan Boundary-Layer Profiles, Report DAC-67086, Douglas Aircraft Company, Santa Monica, CA.

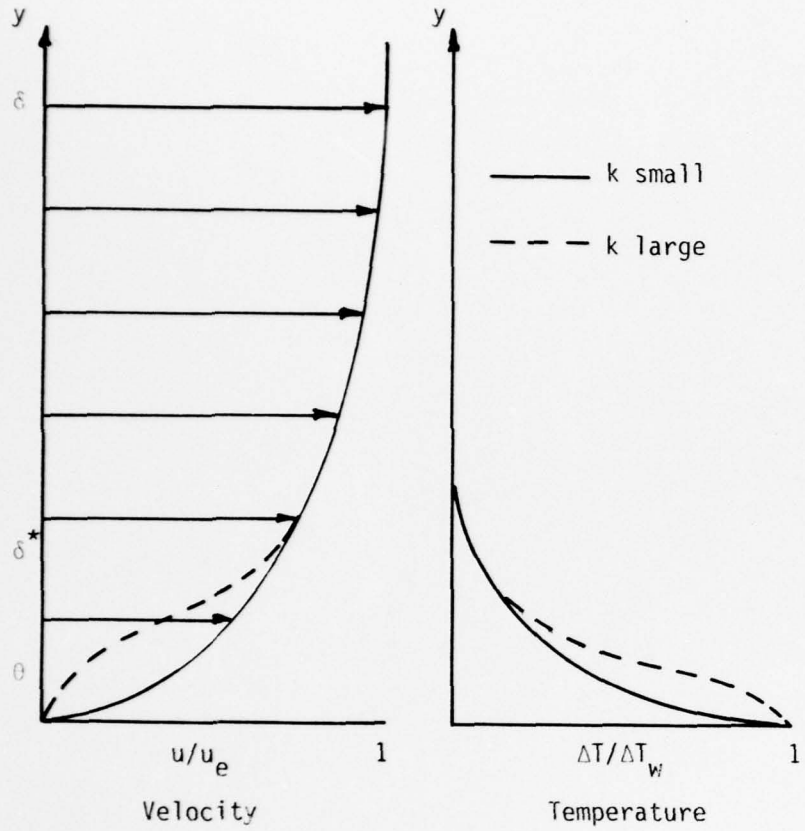

Figure 1. Qualitative Mean Flow Profile

$P_r = \nu/\kappa = O(10)$

$P_t = \varepsilon_M/\varepsilon_H = O(1)$

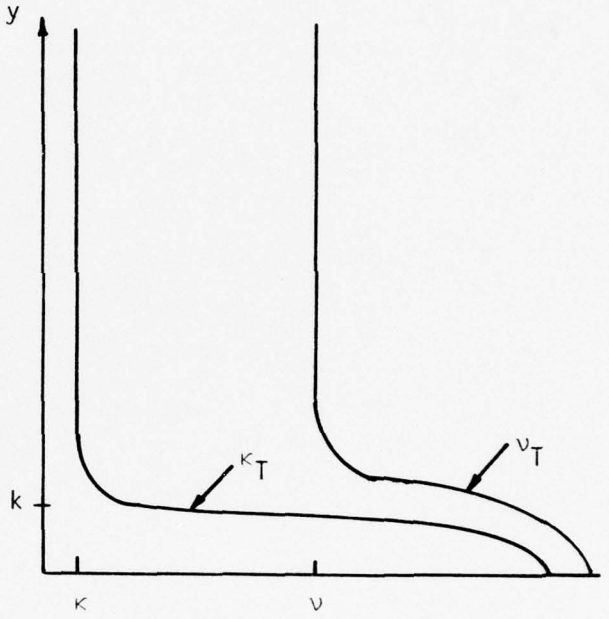

Figure 2. Total Effective Diffusivities (Qualitative)

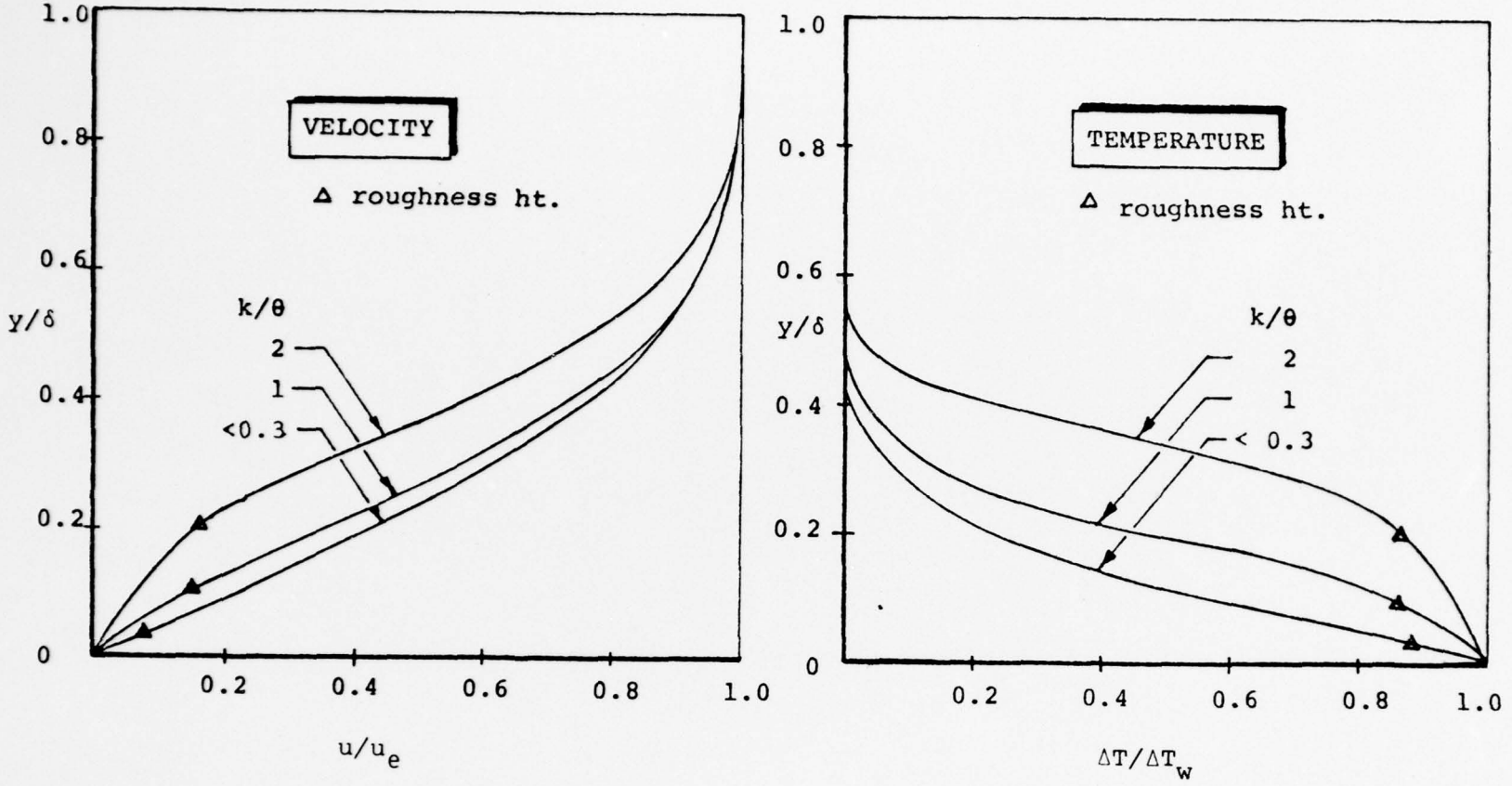

Figure 3. Effect of Roughness on Mean Boundary-Layer Profiles, Zero Pressure Gradient, $\beta = 0$ $Re_\theta = 175$

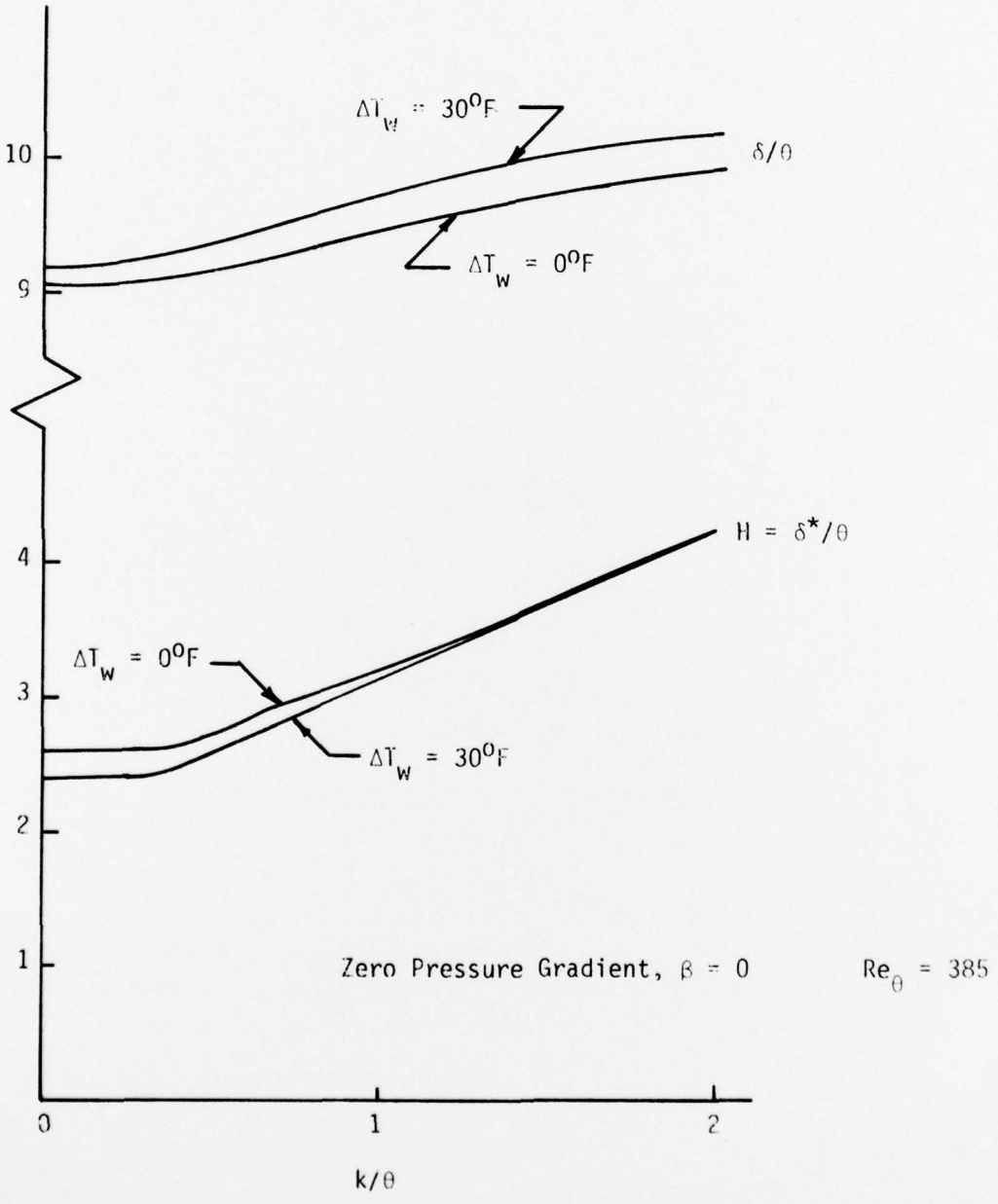

Figure 4. Influence of Effective Roughness Height on Momentum Thickness and Boundary Layer Thickness

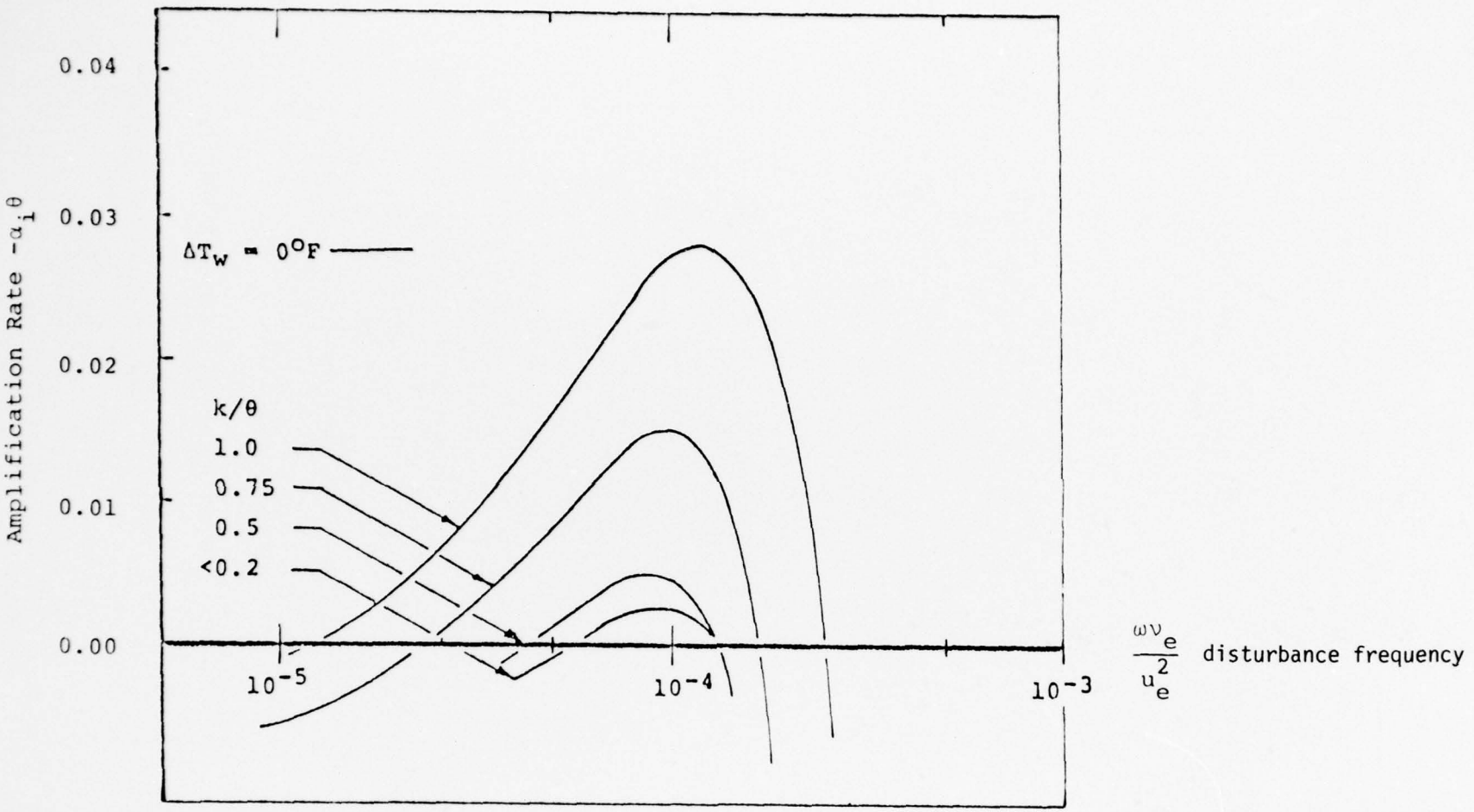

Figure 5. Rough Wall Amplification Rates,
Zero Pressure Gradient, $\beta = 0$ $Re_\theta = 385$

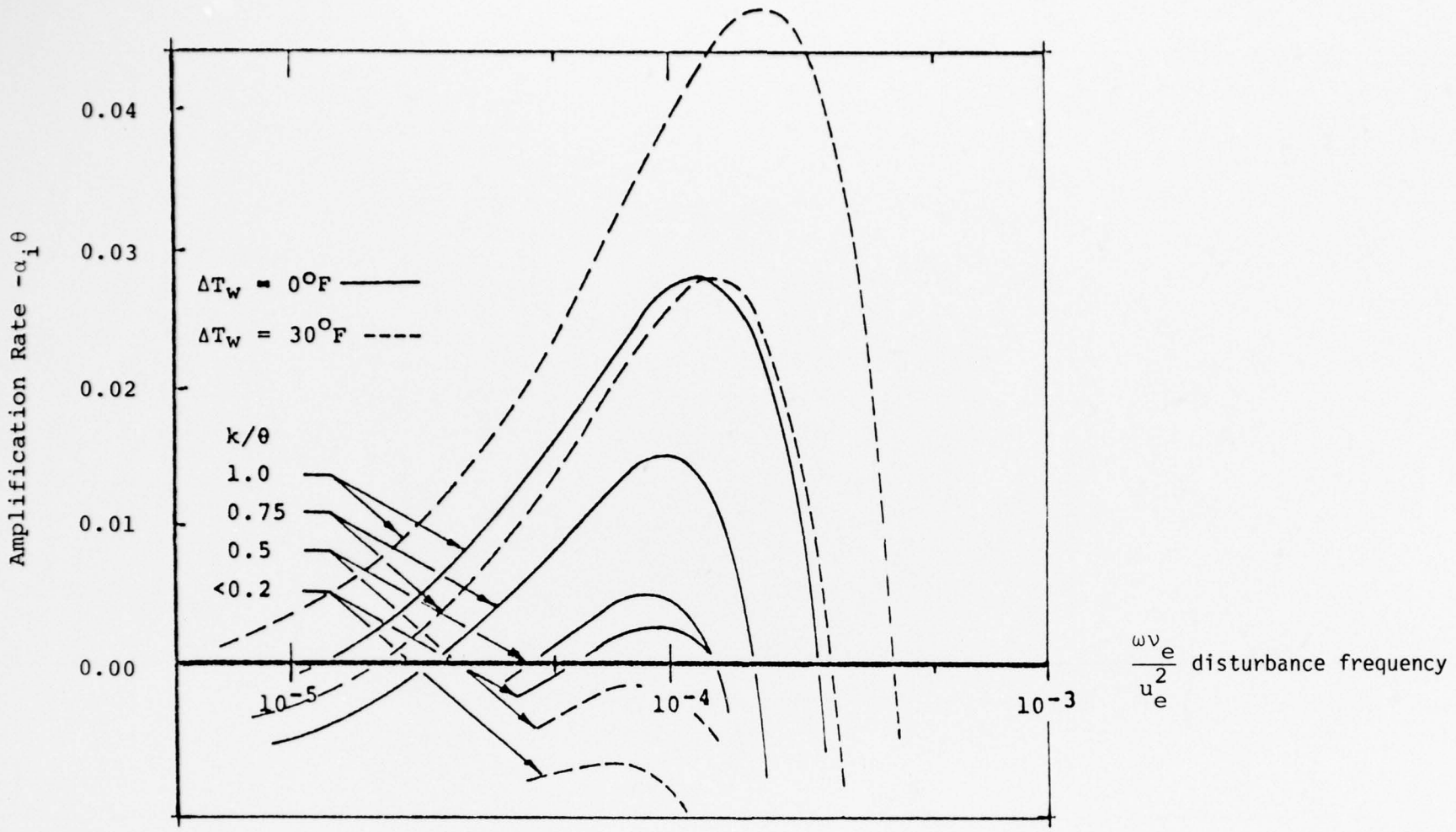

Figure 6. Rough Wall Amplification Rates,
Zero Pressure Gradient, $\beta = 0$ $Re_\theta = 385$

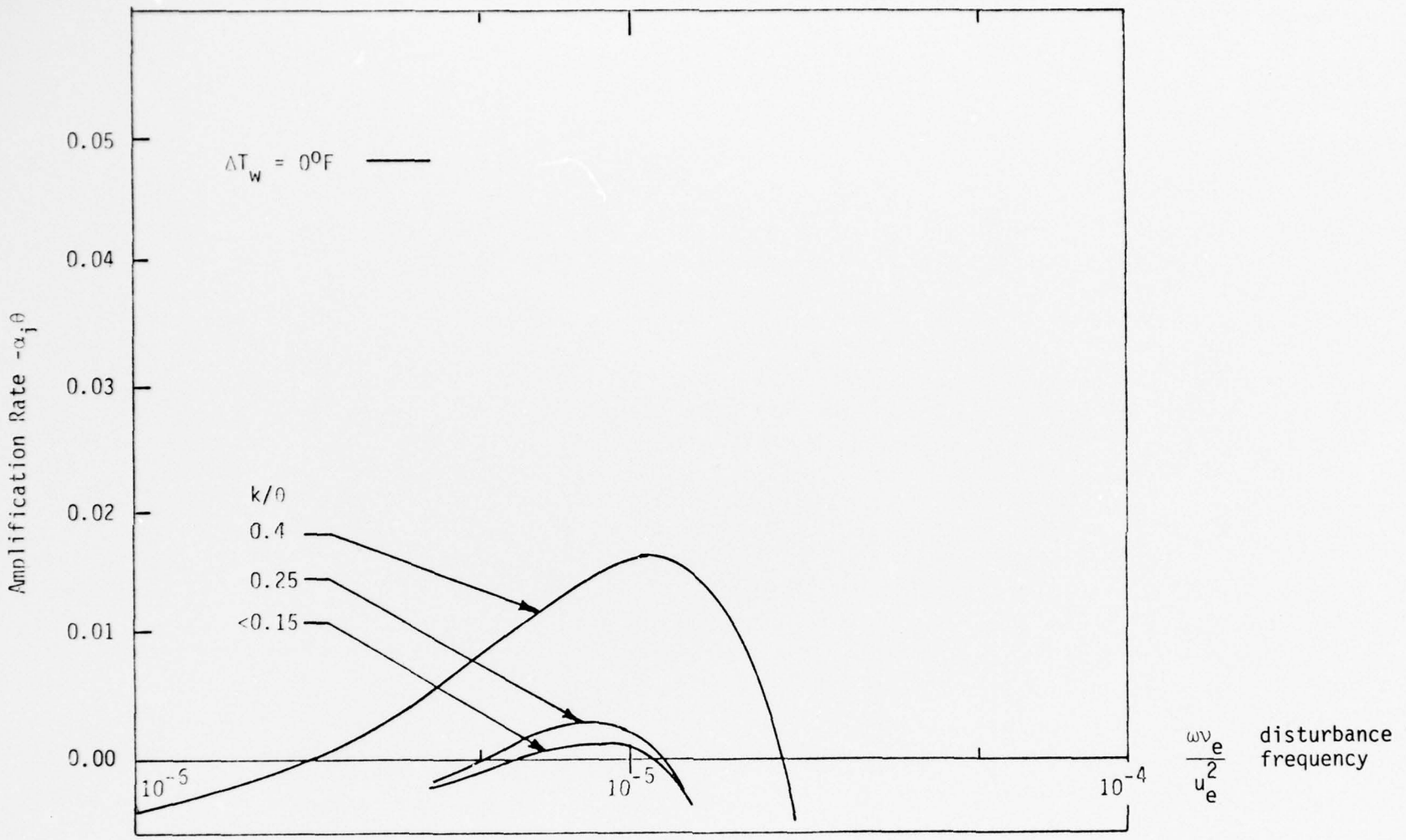

Figure 7. Rough Wall Amplification Rates,
Favorable Pressure Gradient, $\beta = .2$ $Re_\theta = 2103$

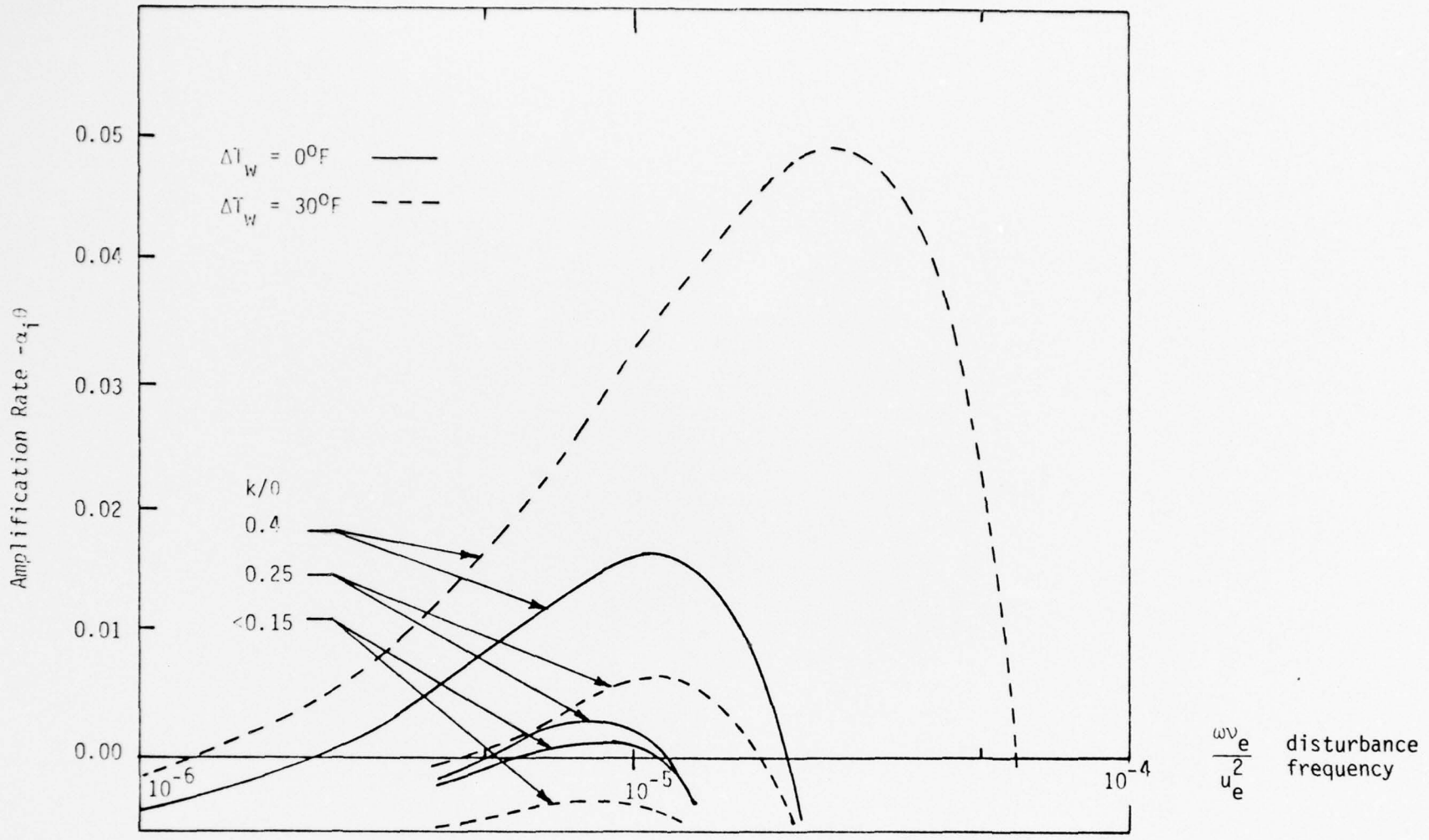

Figure 8. Rough Wall Amplification Rates,
Favorable Pressure Gradient, $\beta = .2$ $Re_\theta = 2103$

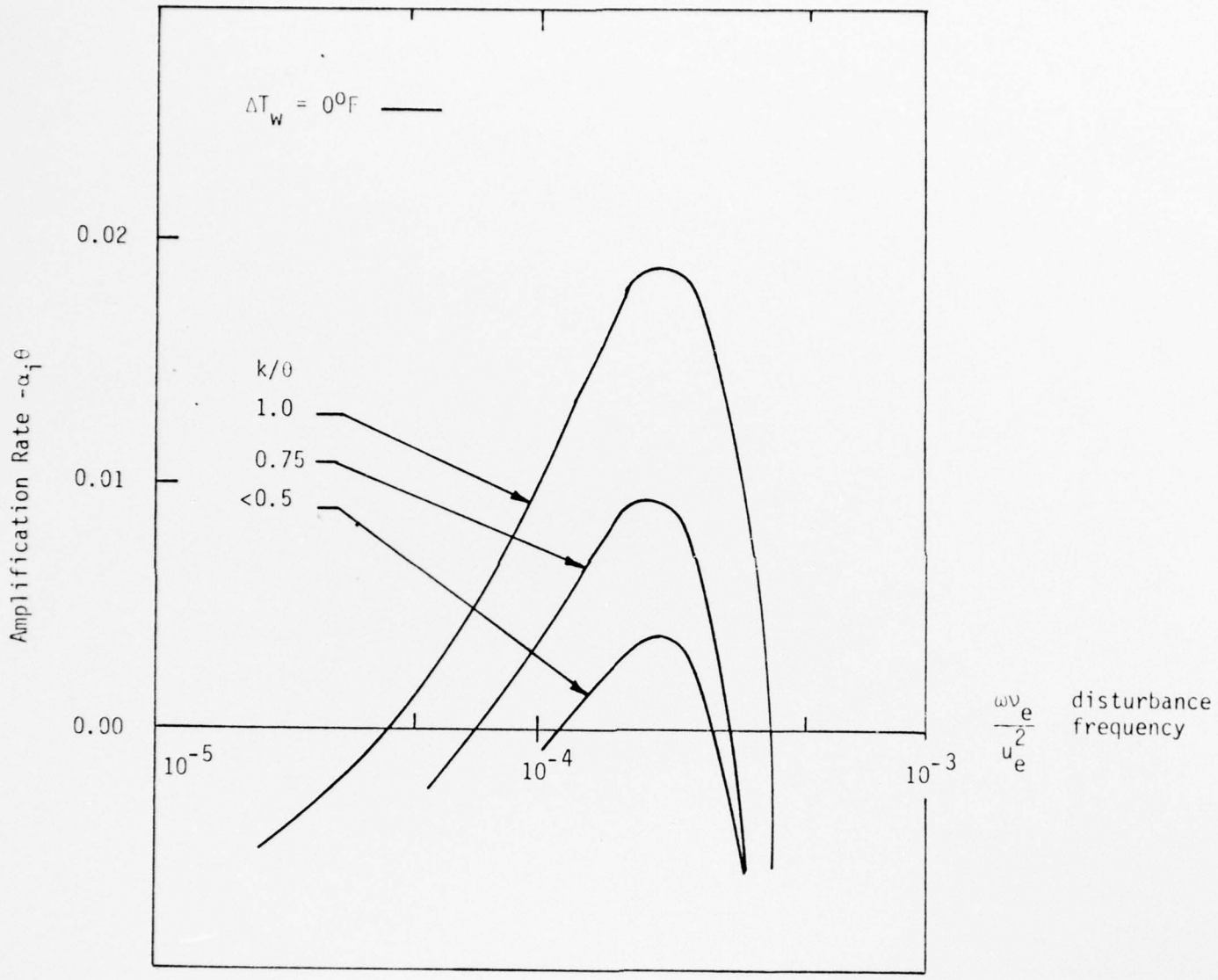

Figure 9. Rough Wall Amplification Rates,
Adverse Pressure Gradient, β = -0.05 Re_θ = 224

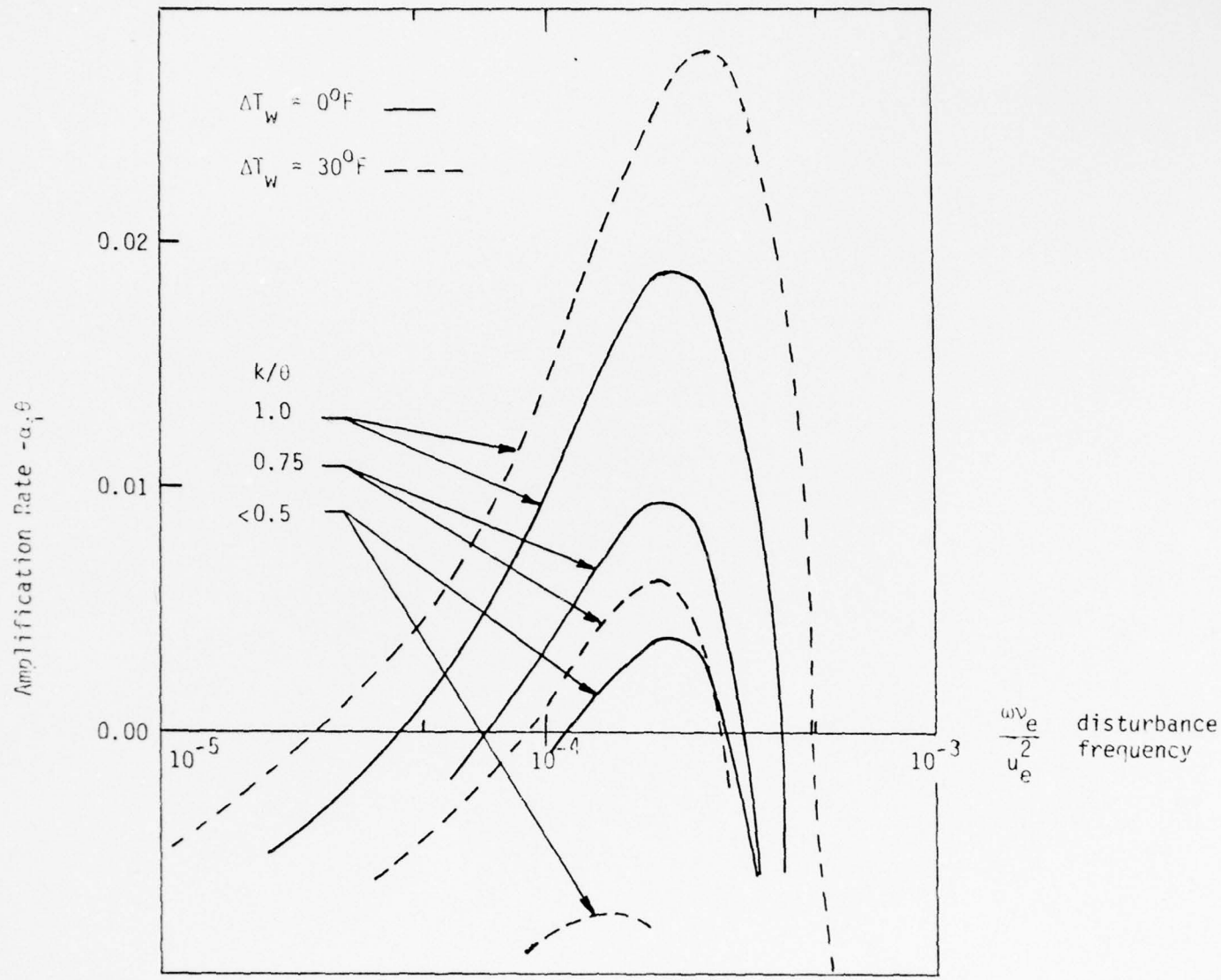

Figure 10. Rough Wall Amplification Rates,
Adverse Pressure Gradient, β = -0.05 Re_θ = 224

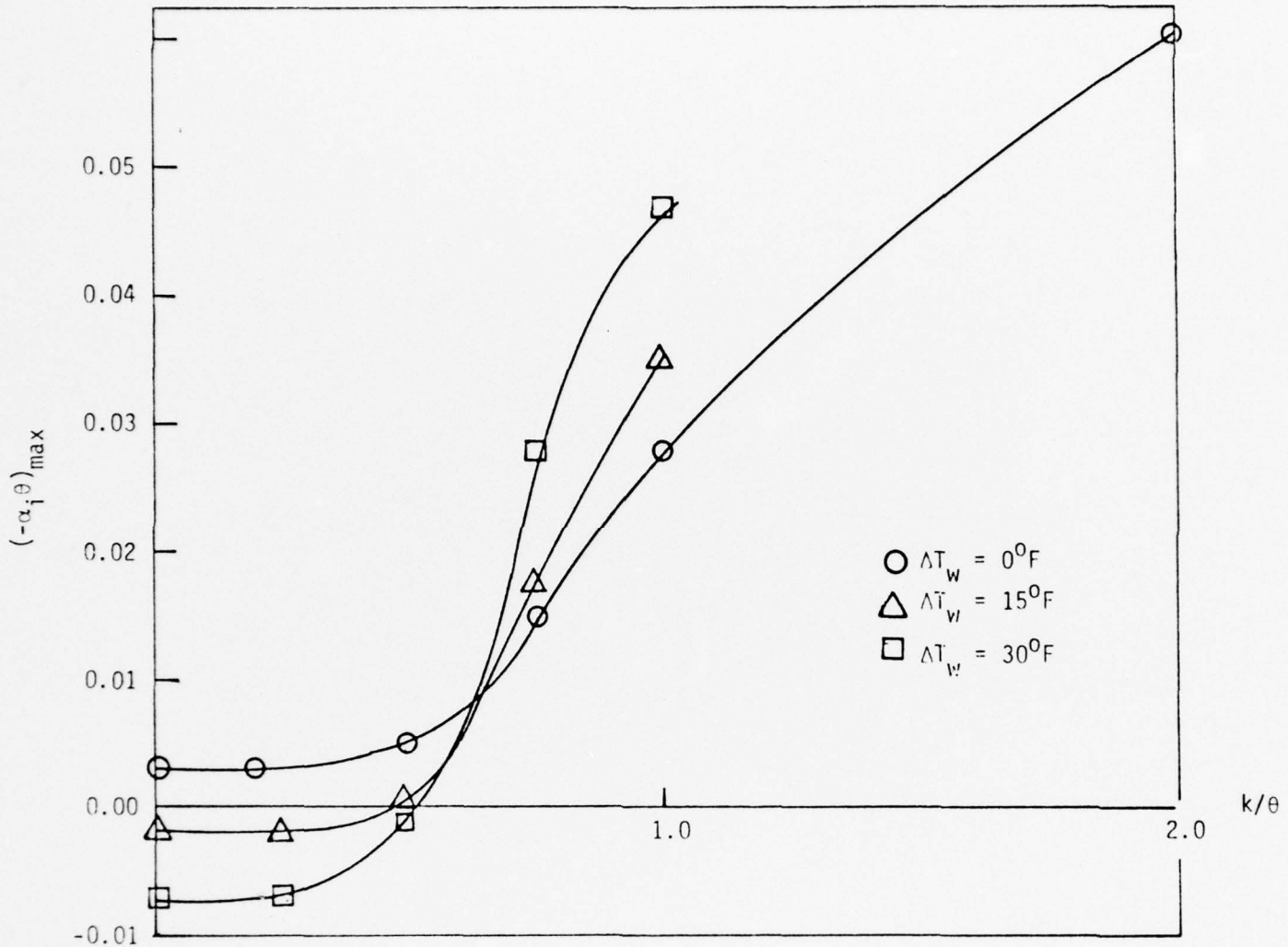

Figure 11. Dependence of Maximum Amplification Rate on Roughness Height, Zero Pressure Gradient, $\beta = 0$ $Re_\theta = 385$

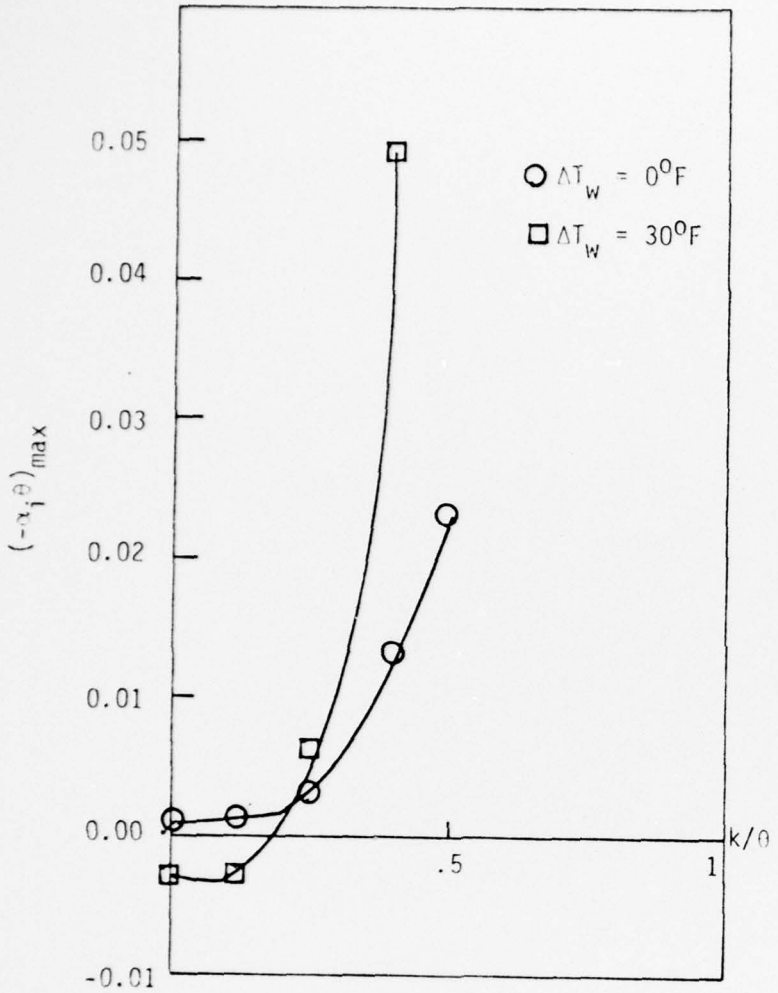

Figure 12. Favorable Pressure Gradient
β = .2 Re_θ = 2103

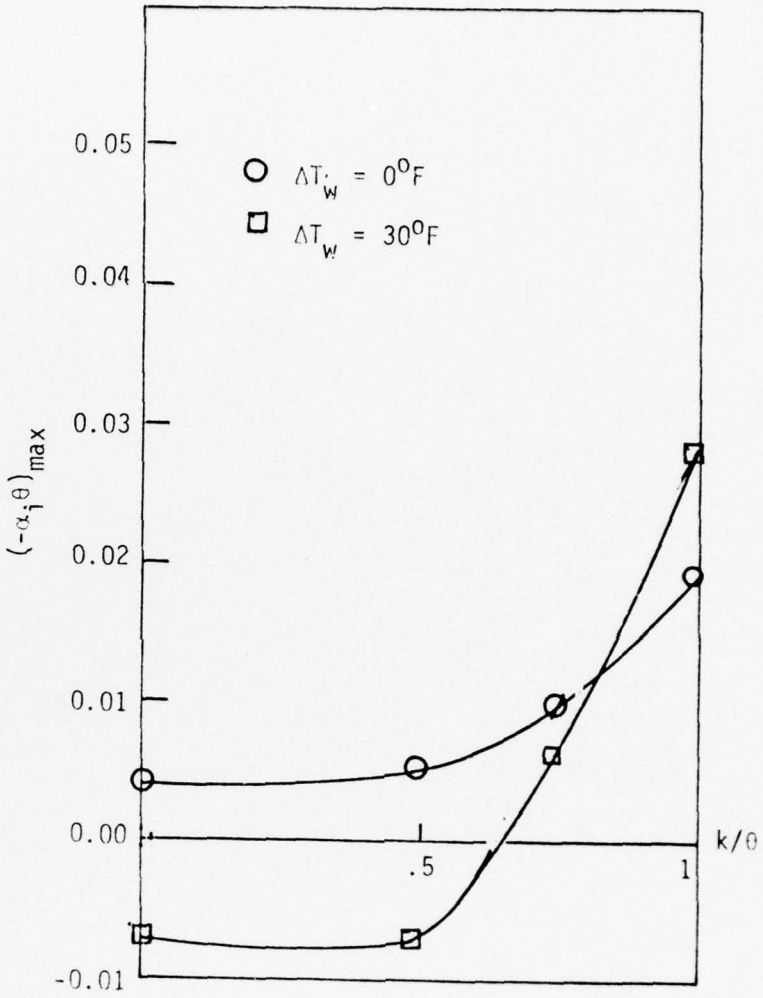

Figure 13. Adverse Pressure Gradient,
β = -0.05 Re_θ = 224

Dependence of Maximum Amplification Rate on Roughness Height

Falkner-Skan Pressure Gradient Parameter, β	$\frac{k}{\theta}$	$\Delta T_w = 0^oF$	$\Delta T_w = 30^oF$
0 Zero pressure gradient	≤.25	Negligible	Negligible
	.5	Small	Moderate
	.75	Drastic	Drastic
-0.05 Adverse pressure gradient	≤.5	Negligible	Negligible
	.75	Moderate	Drastic
	1.0	Drastic	Drastic
0.2 Favorable pressure gradient	≤.15	Negligible	Negligible
	.25	Moderate	Drastic
	.4	Drastic	Drastic

Figure 14. Effect of Roughness on Amplification Rates

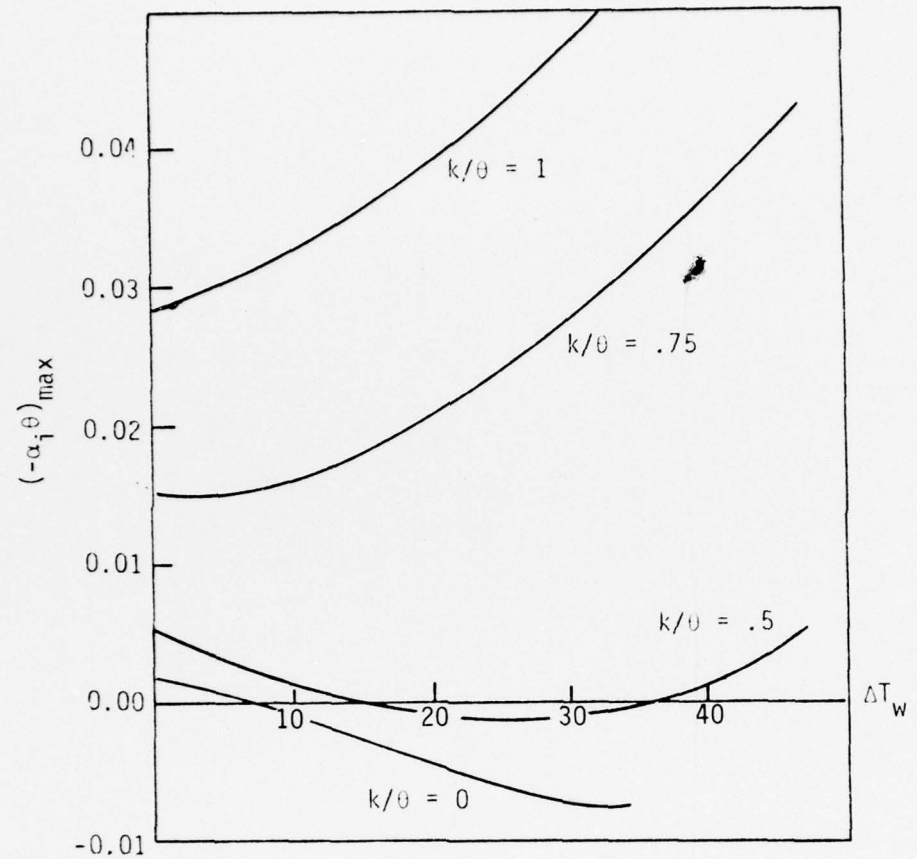

Figure 15. Effectiveness of Heating in the Presence of Roughness, Zero Pressure Gradient, $\beta = 0$ $Re_\theta = 385$

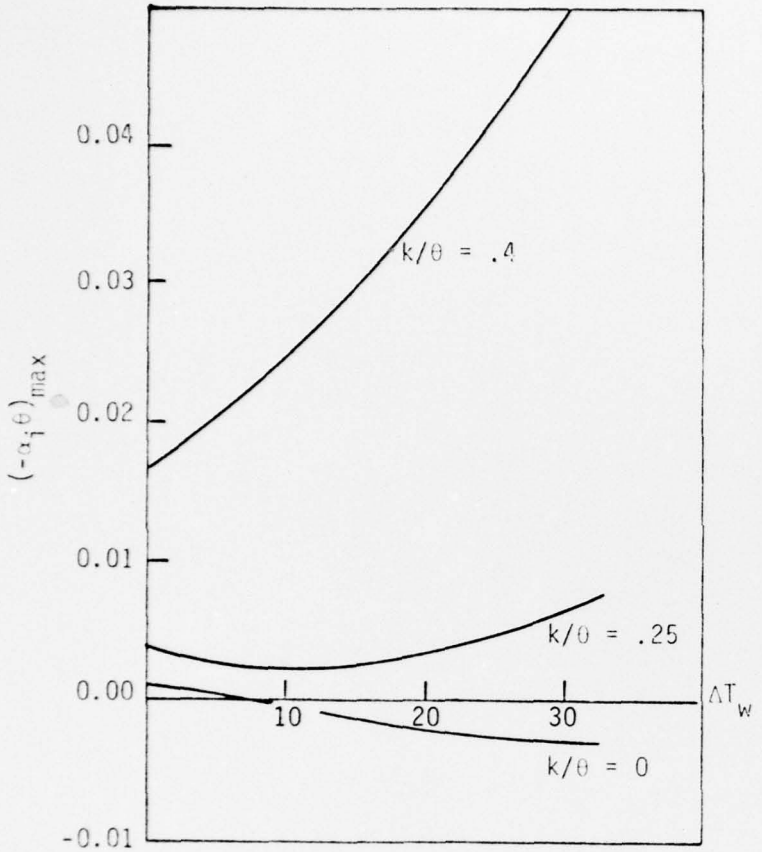

Figure 16. Favorable Pressure Gradient,
β = .2 Re_θ = 2103

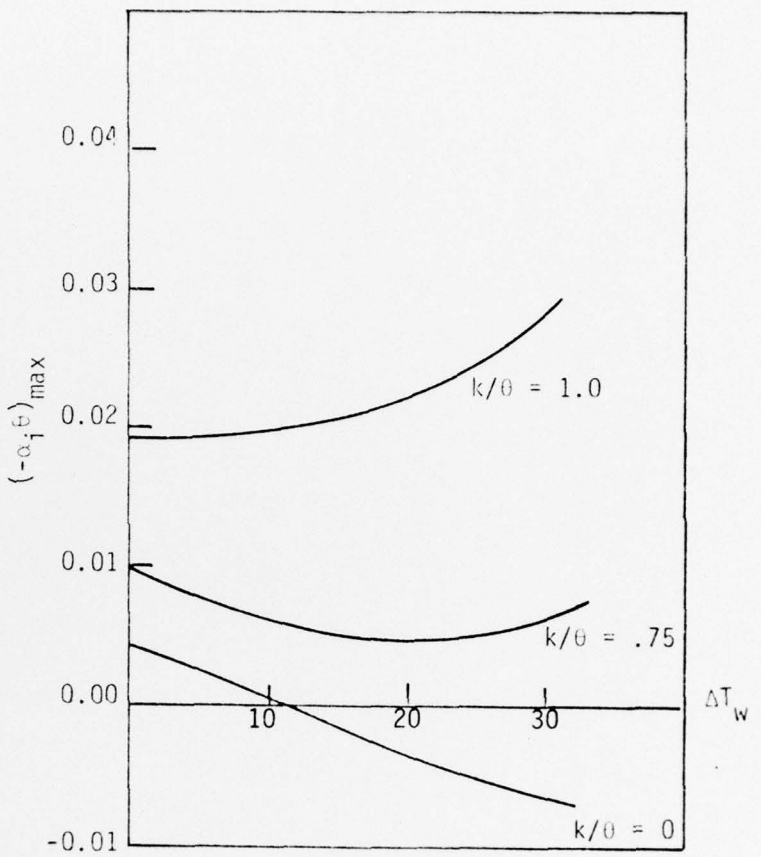

Figure 17. Adverse Pressure Gradient,
β = -0.05 Re_θ = 224

Effectiveness of Heating in the Presence of Roughness